

## 2D and 3D Propagation Modelling with Coupled Modes

E. Noutary and A. Plaisant

Thomson Sintra ASM, Departement de Sophia, 525 route des Dolines,  
BP157, 06903 SOPHIA-ANTIPOLIS Cedex, France

A numerical modelling of two and three dimensional acoustic propagation in inhomogeneous oceans with variations of bottom depth and sound speed profile, based on coupled modes theory is presented.

The model still under development and evaluation called "MOCTESUMA" includes computation in 2D of the direct and backscattered field in the water column as well as in the sediment layer supporting shear waves.

In 3D, a geometrical approach is used to describe transmission and reflection effects in the horizontal plane, but presently, there is no shear in the sediment and in order to achieve reasonable computing time, other simplifying assumptions are made; nevertheless the model has the capability to work with a complex bottom topography described by iso-depth contours. An analysis of the limitations of the model is performed by comparisons with published benchmarks in 2D and by comparisons with other models results in cases of range variable velocity profiles.

*\* This work has been partly funded within the European Community framework of the MAST programme (DG XII).*

### I INTRODUCTION

A first attempt by Thomson Sintra ASM (TS.ASM), France, to model 3D diffraction effects due to propagation over a variable depth ocean was undertaken under the European Community MAST1 project "SNECOW". This effort was carried on under programme MAST2 with the project "PRO.MODE", where this time, the propagation modelling effort was shared with several partners: FORTH in Greece and Technical University of Denmark. Two major techniques to model 3D propagation were examined: the Parabolic Equation and the Coupled Modes method with objective to find respective limitations and validity domain.

This paper presents the principal results obtained by TS.ASM with the Coupled Modes method and concentrates on low frequency shallow water forward and backward propagation effects due to bottom topography, which is known as being the most important effect in shallow waters.

Before going to 3D propagation modelling, it is natural to start investigating the bottom effect in 2D and, in particular, the influence of shear waves in the sediment layers. The main innovation of TS.ASM method is the possibility to compute the backscattered field including shear waves in range variable environment. This is done in paragraphs II to V, starting with the theoretical bases of the Coupled Modes method including shear, to finish with comparisons with other numerical codes in classical configurations such as stratified ocean and fluid bottom variations.

In paragraph VI, the 3D case is considered. Test cases with a sinusoidal bottom for which published results are available are presented. Comparisons are made between these results and two versions of TS.ASM software corresponding to different approximations. Finally, the problems encountered with the method are reported.

### II LINEAR ELASTICITY IN STRATIFIED MEDIA

#### II.1 - Modal expansions.

In this section, concepts and notations used to establish theoretical developments needed for

evaluating the acoustic field in wave guides including shear are presented. All these concepts can be found in details in reference books such as, for example Ewing et al [1] and Brekhovskikh [2]. In order to evaluate the displacement vector  $\underline{U}$  in elastic layers, it is convenient to define a scalar potential  $\phi$  and a potential vector  $\underline{\Psi}$  such that:

$\underline{U} = \nabla\phi + \nabla \wedge \underline{\Psi}$ .  $\phi$  is the compressional potential scalar and  $\underline{\Psi}$  is the shear compressional vector. If coupling between compressional and shear waves due to continuous variations with depth of shear velocity is neglected, the two potentials  $\phi$  and  $\underline{\Psi}$  satisfy wave equations in each layer of the waveguide (see for example Ewing et al [1] and Arvelo et al [6]). Under axisymmetric assumptions and assuming that no SH waves can be excited (in the present work, only the cases of monopolar sources located in the water column are treated), the only interesting component of vector  $\underline{\Psi}$  is  $\Psi_z$  and we can define  $\psi$  such

that:  $\Psi_z = -\frac{\partial\psi}{\partial r}$ . The two potentials  $\phi$  and  $\psi$  are solutions of the wave equations

$$\Delta\phi = \frac{1}{c_p^2} \frac{\partial^2\phi}{\partial t^2} \quad \text{and} \quad \Delta\psi = \frac{1}{c_s^2} \frac{\partial^2\psi}{\partial t^2}$$

In cases of harmonic sources, using a technique of separation of variables and notations defined by Koch et al [3], the potentials  $\phi$  and  $\psi$  may be described as a superposition of depth eigenmodes given by:

$$\phi(r, z) = \sum_n R_n(r) u_n(z) \quad \text{and} \quad \psi(r, z) = \sum_n R_n(r) v_n(z) \quad \text{eq.1}$$

where the range functions  $R_n$  satisfy:  $\frac{1}{r} \frac{\partial}{\partial r} \left( r \frac{\partial R_n}{\partial r} \right) + k_n^2 R_n = 0 \quad (r \neq 0)$

and the depth eigenfunctions satisfy:

$$u_n'' + k_p^2 u_n = k_n^2 u_n \quad \text{and} \quad v_n'' + k_s^2 v_n = k_n^2 v_n$$

Since harmonic sources are considered, dependance in time has been omitted and ' denotes the derivation along variable  $z$ . In the previous expressions  $k_n^2$  denotes the eigenvalue associated with the eigenfunctions  $u_n$  and  $v_n$ ;  $k_p = \omega/c_p$  is the wave number associated with the compressional waves and  $k_s = \omega/c_s$  is the wave number associated with the shear waves

**Expressions of the displacement vector components:** denoting  $q_n$  and  $w_n$  the following quantities:  $q_n = u_n + v_n'$  and  $w_n = u_n' + k_s^2 v_n$ ,

the components of the displacement vector  $\underline{U}$  take following form:

$$U_r = \sum_n q_n \frac{dR_n}{dr} \quad U_z = \sum_n w_n R_n$$

**Expressions stress tensor components used below:** denoting  $p_n$  such that:

$p_n = 2q_n' + k_s^2 v_n$ , components of the stress tensor  $\underline{P}$  used below take the following

form:  $P_{rz} = \rho \omega^2 \sum_n \frac{p_n}{k_s^2} \frac{dR_n}{dr}$  ;

$$P_{zz} = \rho \omega^2 \sum_n \left( -u_n + 2 \frac{k_n^2}{k_s^2} q_n \right) R_n \text{ and } P_{rr} = -\rho \omega^2 \sum_n \left[ \left( q_n + \frac{p_n'}{k_s^2} \right) R_n + \frac{2q_n}{rk_s^2} \frac{dR_n}{dr} \right]$$

Therefore, all physical quantities can be expressed in terms of functions  $u_n$  and  $v_n$  and their derivatives in case of homogeneous stratified media

**Expression of the acoustic field in the water column:** propagation loss for a harmonic source at depth  $z_0$  in the water is given by the usual expression  $20 \log(|p(r, z)|)$  where (see for example Brekhovskikh [2] and Ellis et al [4]):

$$p(r, z) = i \pi \sum_n \frac{u_n(z_0) u_n(z)}{N_n} H_0^1(k_n r)$$

(In the water column no shear wave is excited and the water density is assumed to be 1). The constant normalisation  $N_n$  of the couple of modes  $(u_n, v_n)$  can be obtained using Cauchy's theorem (residues in the complex plane, see for example Ellis et al [4]) or directly if a bilinear form  $\langle \cdot, \cdot \rangle$  satisfying the two following properties:

- 1)  $\langle (\delta(z-z_0), 0), (u_m, v_m) \rangle = u_m(z_0)$  for all  $m$  eq.2
- 2)  $\langle (u_m, v_m), (u_n, v_n) \rangle = 0$  for  $m \neq n$  (orthogonality condition), eq.3

can be founded; in this case we have:  $N_n = \langle (u_n, v_n), (u_n, v_n) \rangle$

In the case of a fluid bottom, the bilinear form is simply the scalar product:

$$\langle u_m, u_n \rangle = \int \rho(z) u_m(z) u_n(z) dz$$

In the case of an elastic bottom, the bilinear form is more complicated because of more complex continuity conditions between layers. Such a bilinear form is derived in next section.

## II.2 Orthogonality condition between modes.

The orthonormalisation condition of a set of eigenfunctions in an elastic wave guide has been established by Auld [5] and Koch et al [3]. The authors assume real values of wave numbers  $k_p$  and  $k_s$  which is not valid if volumic attenuation, which is an important effect, is introduced. Therefore another "closed" condition is derived which turned out to be identical to the one of Ellis et al [4]. The derivation is presented here because it is simple, similar to the fluid bottom case and it helps understanding the Galerkin method used for the case of non homogeneous layers (see section II.3)

**Notations and assumptions:** the wave guide is assumed to be horizontally stratified (a water column overlying sediment layers) bounded at the top ( $z=0$ ) by a free surface and at the bottom ( $z=b$ ) by a perfectly rigid substratum.

$(u_n, v_n)$  denotes a couple of eigenfunctions ( $u_n$  for compressional waves and  $v_n$  for shear waves).

$a(\cdot, \cdot)$  and  $b(\cdot, \cdot)$  denote two symmetric bilinear forms defined by:

$$a(u_m, u_n) = \int_0^b \rho k_p^2 u_m u_n - \rho u_m' u_n' dz \text{ and } b(v_m, v_n) = \int_0^b \rho k_s^2 v_m v_n - \rho v_m' v_n' dz$$

For any given function  $f(z)$  continuous in each layer of the wave guide we define

$$\{f\} \text{ such that: } \{f\} = - \sum_i [f]_{z_i} + f(b) - f(0)$$

where  $[f]_{z_i}$  is the jump of  $f$ ;  $z_i$  is the depth of the  $i^{\text{th}}$  interface;  $b$  is the depth of the bottom of the wave guide.

In order to obtain orthogonalisation expressions, we integrate by parts the expression of  $a$ :

$$0 = a(u_m, u_n) - a(u_n, u_m) = (k_m^2 - k_n^2) \int_0^b \rho u_m u_n dz - \{ \rho u_m' u_n \} + \{ \rho u_n' u_m \}$$

**In the case of fluid bottom**, the terms in brackets are equal to 0 (boundary conditions plus continuity of pressure:  $\rho u_n$  and of the vertical component of displacements vector:  $u_n'$ ). This shows that the orthogonality condition is simply:

$$\int_0^b \rho(z) u_m(z) u_n(z) dz = 0$$

**In the case of elastic layers**, continuity conditions between layers are more complex and additional terms containing value of  $v_n$  and of  $v_n'$  are needed. These terms can be obtained

$$\text{integrating by parts expression of } b: b(v_m, v_n) - k_m^2 \int_0^b \rho v_m v_n dz = - \{ \rho v_m' v_n \}$$

Using the symmetric property of the form  $b$  and noting that  $\rho(u_m w_n - k_m^2 v_n q_m)$  is continuous through each interface, we find:

$$0 = (k_m^2 - k_n^2) \left( b(v_m, v_n) + \int_0^b \rho u_m u_n dz + \{ \rho q_m v_n + \rho v_m q_n \} \right)$$

Integrating by parts, we obtain another expression for this equation:

$$0 = \int_0^b \rho \left( q_m \cdot q_n + \frac{v_m \cdot p_n}{2} + \frac{v_n \cdot p_m}{2} \right) dz \quad \text{for } m \neq n \quad \text{eq.4}$$

If we define a bilinear form by

$$\langle (u_m, v_m), (u_n, v_n) \rangle = \int_0^b \rho \left( q_m \cdot q_n + \frac{v_m \cdot p_n}{2} + \frac{v_n \cdot p_m}{2} \right) dz \quad \text{for } m \neq n$$

we find that this bilinear form satisfies equations 2 and 3. The constant normalisation is then:

$$N_n = \int_0^b \rho \left( q_n^2 + v_n \cdot p_n \right) dz \quad \text{eq.5}$$

**Remark:** Koch et al [3] find an orthonormalisation condition of the form:

$$J(u_m, v_m; u_n, v_n) = \int_0^b \rho \left( q_m \cdot q_n^* + \frac{v_m \cdot p_n^*}{2} + \frac{v_n \cdot p_m}{2} \right) dz$$

( $\delta_{mn}$  denotes the Kronecker symbol). This expression is identical to expression 4 for real eigenfunctions. Let us examine the case of complex eigenfunctions. For real  $k_s$  and denoting  $f^*$  the complex conjugate of a function  $f$ , the function  $(u_m w_n^* - k_m^2 v_n^* q_m) \cdot \rho$  is continuous through each interface. Under this assumption similar calculations than the ones presented in this section lead to:

$$\int_0^b \rho (k_p^2 - k_p^{*2}) u_m u_n^* dz = (k_m^2 - k_n^{*2}) J(u_m, v_m; u_n, v_n)$$

Then, if  $k_p$  is not real, orthonormalisation condition defined with  $J$  may fail.

Equation 4 does not define an orthonormalisation condition because values of the bilinear form  $\langle \cdot, \cdot \rangle$  may be complex. Nevertheless, as it is shown in the paper published by Ellis et al [4], the proper definition of the constant  $N_n$  is the complex value defined in equation 5.

### II.3 A Galerkin method for inhomogeneous layers.

In cases of vertical dependence of the sound speeds  $c_p = c_p(z)$  and  $c_s = c_s(z)$  in each layer, the search for eigenvalues and eigenfunctions is achieved through the following procedure:

- We first assume that we have already calculated the orthonormal set of eigenfunctions  $(u_{cm}, v_{cm})$  associated with the homogeneous layers case such that the two constant values of compressional and shear waves speed in the  $j^{th}$  layer ( $c_{pj}$  and  $c_{sj}$ ;  $z_{j-1} < z < z_j$ ), are given by:

$$\rho(z_j^+)c_{sj+1}^2 - \rho(z_j^-)c_{sj}^2 = [\rho.c_s^2]_{z_j} \quad \text{and} \quad c_{pj+1} = c_p(z_j^+) \quad (z_0=0) \quad \text{eq.6}$$

$[\rho.c_s^2]$  denotes the jump of the depth function  $\rho(z).c_s^2(z)$ .  $k_{sc}$  and  $k_{pc}$  denote the wave numbers associated with these sound speed profiles (constant in each layer).

- The calculation of the eigenfunctions  $(u_i, v_i)$  and eigenvalues  $k_i^2$  associated with the complete problem is achieved by expanding them on the basis of the eigenfunctions  $(u_{cm}, v_{cm})$  already calculated and the eigenvalues of which are  $k_{cm}$ .

Denoting  $q_{cm}, w_{cm}$  and  $p_{cm}$  the following quantities:

$$q_{cm} = u_{cm} + v'_{cm} \quad ; \quad w_{cm} = u'_{cm} + k_{cm}^2 v_{cm} \quad \text{and} \quad p_{cm} = 2q'_{cm} + k_{sc}^2 u_{cm} ,$$

each eigenfunction in layers containing compressional and shear waves has to be described as a couple of eigenmodes. The modal expansion of  $(u_i, v_i)$  is expressed as follows:

$$(u_i, v_i) = \sum_{n_i} a_{n_i} (u_{cn}, v_{cn}) \quad \text{Using the same technique than the one presented in section}$$

II.2, and the continuity of  $\rho(u_{cm}w_i - k_{cm}^2 v_i q_{cm})$  and  $\rho(u_i w_{cm} - k_i^2 v_{cm} q_i)$  at each horizontal interface the search of eigenfunctions  $(u_i, v_i)$  and eigenvalues  $k_i^2$  associated with the case of a horizontally stratified waveguide with heterogeneous layers reduces to the search of the  $i^{th}$

eigenvector  $\{a_{ni}\}$  and eigenvalue  $k_i^2$  of the matrix  $(M_{mn} + k_{cm}^2 \delta_{mn})$  with:

$$M_{m,n} = \int_0^b \rho (k_p^2 - k_{pc}^2) u_{cm} u_{cn} dz + k_{cm}^2 \int_0^b \rho (k_s^2 - k_{sc}^2) v_{cm} v_{cn} dz \quad \text{eq.7}$$

## III A 2 WAY COUPLED MODES TECHNIQUE INCLUDING SHEAR

### IN NON STRATIFIED MEDIA.

Like in the case of a fluid bottom, the mode coupling technique is obtained by using the orthogonality condition of mode families associated with two horizontally stratified subdomains  $\Omega_1$  and  $\Omega_2$  and writing the continuity of physical quantities. In the case of elasticity,  $U_r, P_{rz}, P_{rz}$  are continuous along the vertical boundary between the two subdomains and  $U_z$  is continuous in the sediment layer.

#### III.1 Assumptions.

In order to extend the mode coupling technique to include shear waves, we first begin to make a far-field approximation: we will neglect terms decaying as  $1/r$  in range (compared

with terms decaying as  $1/\sqrt{r}$ ). Then  $\frac{2q_n}{rk_s^2} \frac{dRn}{dr} \approx 0$  in expression of  $P_{rz}$  (section

II.1). Moreover, under this assumption, Hankel functions can be approximated with exponential functions.

#### III.2 Use of orthogonality condition to derive coupling matrices.

In the far field approximation, the "orthonormality" condition gives:

$$\int_0^b \left[ P_{xz} Q_n - \rho \omega^2 U_z \frac{P_n}{k_s^2} \right] dz \approx -\omega^2 R_n ; \quad \int_0^b \left[ P_{xz} w_n + \rho \omega^2 U_z \left( Q_n + \frac{P_n'}{k_s^2} \right) \right] dz \approx \omega^2 \frac{dR_n}{dz} \quad \text{eq.8}$$

**These two equations are the basic relations of the 2-Way coupled modes method**

In order to obtain these relations, we use the modal expansions of  $P_m, P_{rz}$ ,  $U_r$  and of  $U_z$ . An easy way to obtain previous results is to note that:

$$Q_n' = \frac{1}{2} P_n - \frac{k_s^2}{2} v_n ; \quad w_n = \frac{1}{2} P_n + \frac{k_s^2}{2} v_n \quad \text{and} \quad \int_0^b \rho \frac{P_n'}{k_s^2} U_z dz = - \int_0^b \rho^2 \frac{P_n}{k_s^2} U_z' dz$$

### III.3 - Expressions of coupling matrices.

In this section we derive an expression of the backscattered and transmitted fields due to a single vertical discontinuity of the wave guide located at a range  $r_0$ .

**Notations:** let us denote  $\Omega_j$  and  $\Omega_{j+1}$  two subdomains of the wave guide,  $z_j$  and  $z_{j+1}$  are the respective depths of water columns associated with ( $z_j > z_{j+1}$ ). In order to distinguish the subdomain in which are developed the following calculations, all the quantities previously defined will now be indexed by  $j$ . In order to simplify the following expressions, we respectively define vectors  $A_j, B_j$  the components of which are given by:

$$R_{nj}(r_0) \approx \alpha_{nj}(r_0) e^{ik_{nj}r_0} + \beta_{nj}(r_0) e^{-ik_{nj}r_0} = A_{nj} + B_{nj}$$

$$\frac{dR_{nj}}{dr}(r_0) \approx ik_{nj}(\alpha_{nj}(r_0) e^{ik_{nj}r_0} - \beta_{nj}(r_0) e^{-ik_{nj}r_0}) = ik_{nj}(A_{nj} - B_{nj})$$

**Coupling matrices:** in the case of a vertical discontinuity in the wave guide, a backscattering wave arises. Using the far field assumptions, writing the continuity of  $P_m, P_{rz}$  and of  $U_r$  along the depth interface, noting that  $U_z$  is continuous in the sediment layer, and using equation 8 we can define four coupling matrices  $M_1, M_2, M_3$  and  $M_4$  such that:

$$A_j + B_j = M_1 [A_{j+1} + B_{j+1}] \quad A_{j+1} + B_{j+1} = M_2 [A_j + B_j] \quad \text{eq.9}$$

$$A_j - B_j = M_3 [A_{j+1} - B_{j+1}] \quad A_{j+1} - B_{j+1} = M_4 [A_j - B_j]$$

the coefficients of which are:

$$M_{1,nm} = \int_0^b dz \left[ \rho_{j+1} Q_{mj+1} Q_{nj} - \frac{\rho_{j+1}}{k_{sj+1}^2} P_{mj+1} Q_{nj}' \right] + \int_{z_j}^b dz \frac{\rho_j}{k_{sj}^2} w_{mj+1} P_{nj}$$

$$M_{2,nm} = \int_0^b dz \left[ \rho_j Q_{mj} Q_{nj+1} + \frac{\rho_{j+1}}{k_{sj+1}^2} w_{mj} P_{nj+1} \right] - \int_{z_j}^b dz \frac{\rho_j}{k_{sj}^2} P_{mj} Q_{nj+1}'$$

$$M_{3,nm} = \frac{k_{mj+1}}{k_{nj}} M_{2,mn} \quad \text{and} \quad M_{4,nm} = \frac{k_{mj}}{k_{nj+1}} M_{1,mn}$$

**Remark:** in the case of a fluid bottom, expressions of the coupling matrices reduce to the ones classically obtained (see ref [7],[8] and [9]).

Like in the fluid case, equation 9 show that a good evaluation of the inverse of matrix  $M_1$  is  $M_2$  and then, a similar technique than the one used in the fluid case can be used to evaluate the reflection and transmission matrices. By definition of transmission and reflection matrices, we want to determine the matrices  $R_1, T_1$  such that  $B_j = R_1 \cdot A_j$  and  $A_{j+1} = T_1 \cdot A_j$  when  $B_{j+1} = 0$  and  $R_2, T_2$  so that  $A_{j+1} = R_2 \cdot B_{j+1}$  and  $B_j = T_2 \cdot B_{j+1}$  when  $A_j = 0$ . Because  $R_1$  and  $R_2$  are an extended

"reflection coefficient", it follows that all the modulus of their eigenvalues lie in the interval  $[0,1]$ . So we evaluate  $R_1$  using the inverse of the matrix  $R_1' = I + R_1$  and we obtain:

$$R_1 = 2.(I + M_3 M_2)^{-1} - I \quad \text{and} \quad T_1 = M_2 (I + R_1)$$

$$R_2 = I - 2.(I + M_2 M_3)^{-1} \quad \text{and} \quad T_2 = M_1 (I + R_2)$$

#### IV 2D NUMERICAL APPLICATIONS

##### IV.1 horizontally stratified media.

As it has been presented in section II-3, in cases of depth dependence of the sound speeds  $c_p = c_p(z)$  and  $c_s = c_s(z)$ , eigenfunctions are expanded on a basis of reference mode functions. In the actual version of our numerical code, the reference mode functions are the ones associated with a two layered wave guide (homogeneous water column and sediment layer) bounded, at the top, by free surface and, at the bottom, by a rigid substratum.

Knowing that perturbation techniques fails for taking into account attenuation effects in case of propagation in elastic media (see [8]), the Galerkin method described above is also used for solving this problem (attenuations effects may be introduced by adding depth dependent imaginary parts to  $c_p$  and  $c_s$ ).

**Propagation over an homogeneous sediment layer:** many tests of our model MOCTESUMA have been successfully performed against output from SAFARI and W+IEFL codes (see [8] and [10]). A representative example taken from reference [4] is presented below:

Source: frequency 64 Hz, depth 37 m. Receivers from 0 to 25 km depth 72 m

Water column: sound speed constant from 0 to 28 meters (1508 m/s) and from 45 to 104 meters (1494 m/s) with a linear transition.

Sediment layer homogeneous and infinite; density 2.2; compressional sound speed: 2400 m/s, compressional attenuation: 0.24 dB/ $\lambda$ ; results for 3 values of shear sound speed 1000 m/s; 1100 m/s; 1200 m/s; shear attenuation 1dB/ $\lambda$ .

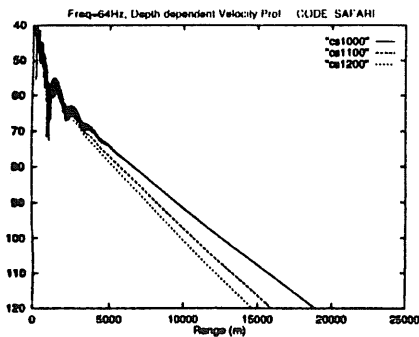


figure 1

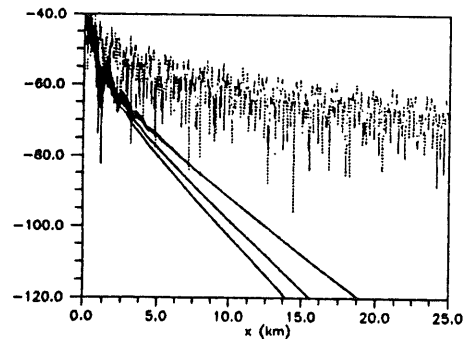


figure 2

figure 1 displays SAFARI results while figure 2 display MOCTESUMA results.

These results are typical of propagation over elastic sediment layers in presence of constant or downward refracting velocity profiles in the water column: transmission losses may become considerable (dashed curve in figure 2 represents transmission losses considering chalk basement). As it is shown in figure 1, results are very sensitive to shear speed in the sediment: if we consider transmission losses up to 100 km as it is the case in published paper [4], variations from 1000 m/s to 1200 m/s of shear speed induces variations of about 110 dB

in transmission losses (from -360 dB to -470 dB)! These variations are depending on the source frequency: same variations of shear speed induces variations (at 100 km in range) of about 40 dB in transmission losses at 128 Hz (from -180 dB to -224 dB) and of about 10 dB at 256 Hz (from -120 dB to -130 dB). Moreover, when running MOCTESUMA with no attenuation in shear, transmission losses are comparable to the fluid case.

**Propagation over inhomogeneous sediment layers:** Galerkin method has been successfully used to take into account variations of sound speed in the water column and attenuation effects in both water and sediment layers. Since to our knowledge, there is no published reference solution for the case of non constant velocity profiles in sediment supporting shear waves, we take, with MOCTESUMA, a sediment layer with a sharp variation of compressional and shear velocities and compare with SAFARI results, replacing the single sediment layer by two isospeed layers, the transition being at the depth of the strong gradient in the MOCTESUMA layer. The following example comes from the SAFARI user's guide [10]

Source: 30 Hz, depth 50 m. Receivers from 0 to 5 km depth 100 m

Water column: sound speed profile 1500 m/s at 0m, 1480 at 30 m, 1490 at 100 m with a linear transitions.

Sediment layer 1: homogeneous; density 1.8; thickness 20 m; compressional sound speed: 1600 m/s, compressional attenuation: 0.2 dB/ $\lambda$ ; shear sound speed 400 m/s; shear attenuation 0.5 dB/ $\lambda$ .

Sediment layer 2: homogeneous and infinite density 2; compressional sound speed: 1800 m/s, compressional attenuation: 0.1 dB/ $\lambda$ ; shear sound speed 600 m/s; shear attenuation 0.2 dB/ $\lambda$ .

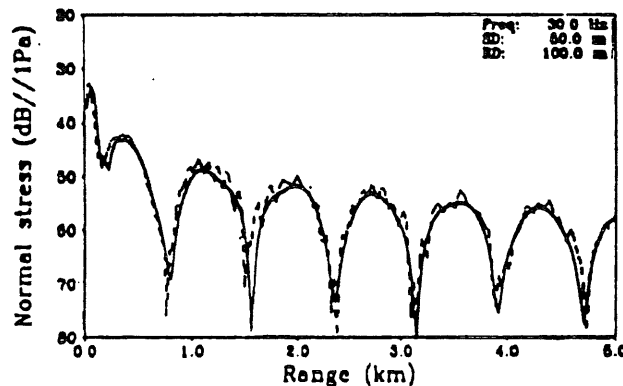


figure 3

On figure3, the continuous curve represents SAFARI results while MOCTESUMA results are plotted with the dashed curve. In order to obtain these results the reference eigenfunctions are the ones associated with the following 2-layered wave guide:

- Water column: constant sound speed 1500 m/s.
- Sediment layer : homogeneous; density 1.8; compressional sound speed: 1600 m/s, compressional attenuation: 0.2 dB/ $\lambda$ ; shear sound speed 400 m/s; shear attenuation 0.5

dB/ $\lambda$ .

Results presented here indicates that the Galrkin method described in section II-3 can be succesfully applied for even strong variations of sound speed profiles.

#### IV. 2 Backscattered field in non stratified media.

We consider now the backscattering from a variable depth bottom consisting of a simple stair step. The fluid parameters are the same as in the stair step case of "Benchmark solutions for backscattering in simple wave guide geometries" published by F.B.Jensen et al [12]:

deepest water depth	200 m	
size of the step	50 m (located at 1.5 km of the source)	
compressional speed	1500m/s in the water	1700m/s in the sediment
density	1 in the water	1.5 in the sediment
attenuation (in compression)		0.5 dB/ $\lambda$ in the sediment

##### Shear parameters in sediment layer:

shear speed	800m/s	attenuation (in shear)	0.5 dB/ $\lambda$
-------------	--------	------------------------	-------------------

The source is a monopole located at an immersion of 100 meters (frequency: 25 Hz). Because, to our knowledge, no reference result including shear waves has been published, we only compare the backscattered field obtained with and without shear in the sediment in figures 4 and 5 (receiver depth 50 m on figure 4 and 170 m on figure 5).

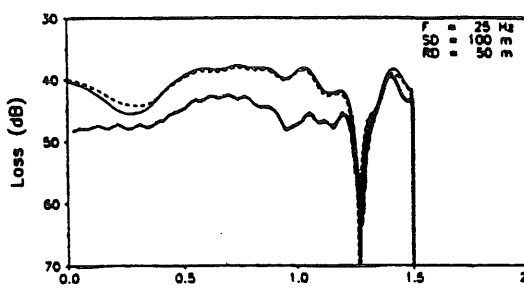


figure.4

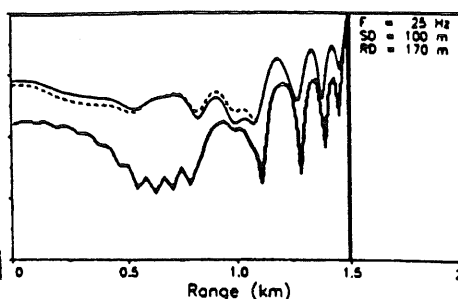


figure.5

In both cases, the two curves which are very similar represent the published results (fluid case - coupled mode method and boundary element method), the third curve displays backscattered field in presence of shear. We can notice that, near the obstacle, the structure of the reflected field is the same in both cases (with and without shear). In order to obtain this results, care have to be taken: in presence of shear in the sediment, the structure of the reflected field is very sensitive to the number of modes used (all the propagative modes have to be calculated) especially when the shear speed in the sediment is small.

## V 3D EXTENSION FOR FLUID SEDIMENT LAYERS

### V.I Description of the method.

When the horizontal wave number vectors  $\underline{\lambda}$  of the incident sound field are not perpendicular to the bottom steps, the problem becomes three dimensional and horizontal deviations are to be expected on the transmitted and reflected field. These horizontal deviations will be accounted for in new reflection and transmission matrices as explained below.

By analogy with the classical plane wave, we will call "horizontal plane wave" carried by the

single vertical mode  $\Psi_n$ , the solution of the Helmholtz equation which can be written as

$$P(x, y, z) = a_n e^{i\lambda_n \cos \theta_i x} e^{i\lambda_n \sin \theta_i y} \Psi_n(z)$$

In order to describe the reflection and transmission phenomena over a bottom step, we first consider the case of an incident plane wave impinging the frontier of the subdomain  $\Omega_2$  with an horizontal grazing angle  $\theta_i$ . The frontier is assumed infinite and straight along axis  $y$ ;  $z$  denotes the variable associated with depth variations.  $P_i$ ,  $P_r$  and  $P_t$  are respectively denoting the incident, reflected and transmitted waves:

$$P_i(x, y, z) = a_n e^{i\lambda_n (\sin \theta_i x + \cos \theta_i y)} \Psi_n(z)$$

$$P_r(x, y, z) = \sum_m b_m e^{-i\lambda_{mx} x + i\lambda_{my} y} \Psi_m(z) \quad P_t(x, y, z) = \sum_k c_k e^{i(\mu_{kx} x + \mu_{ky} y)} \Phi_k(z)$$

Continuity of the Fourier transform along variable  $y$  of the Helmholtz equation indicates that the wave numbers associated with the variable  $y$  must be equal for  $P_i$ ,  $P_r$  and  $P_t$ , so that,  $\theta_m$  denoting the grazing angle associated with the reflected plane wave carried by the mode  $\Psi_m$  (associated with the horizontal wave number  $\lambda_m$  such that  $\lambda_m^2 = \lambda_{mx}^2 + \lambda_{my}^2$ ) and  $\theta_k$  the grazing angle associated with the reflected wave carried by the mode  $\Phi_k$  (associated with the

horizontal wave number  $\mu_k$  such that  $\mu_k^2 = \mu_{kx}^2 + \mu_{ky}^2$ ), should be as:  $\frac{\lambda_n}{\mu_k} = \frac{\cos \theta_{xm}}{\cos \theta_i}$  and

$$\frac{\lambda_n}{\mu_k} = \frac{\cos \theta_{tk}}{\cos \theta_i} \quad \text{The ratio of the horizontal wave number associated with the incident}$$

plane wave and the horizontal wave number associated with the part of the reflected wave carried by the  $m^{\text{th}}$  mode is equal to the ratio of the cosines of the grazing angles of the incident plane wave and the plane wave carried by the  $m^{\text{th}}$  mode of the reflected field. The same observation may be done in the case of the transmitted field.

Like in the 2D case, in order to evaluate the coupling matrices, let us define the vectors  $A, B$  and  $C$  by their elements:  $a_m \cdot e^{i\lambda_n \cos \theta_i \cdot y} \cdot e^{i\lambda_n \sin \theta_i \cdot x_0} \cdot \delta_{mn}$  ( $n$  is the incident mode number),  $b_m \cdot e^{i\lambda_n \cos \theta_i \cdot y} \cdot e^{-i\lambda_{mx} \cdot x_0}$  and  $c_k \cdot e^{i\lambda_n \cos \theta_i \cdot y} \cdot e^{i\mu_{0m} \cdot x_0}$ .

We also define matrix  $D_A$  the only non nul coefficient of which is  $(D_A)_{nn} = i\lambda_n \sin \theta_i$

and two matrices  $D_B$  and  $D_C$  such that:  $(D_B)_{ml} = -i\lambda_{mx} \delta_{ml}$ ;  $(D_C)_{ml} = i\mu_{mx} \delta_{ml}$ .

Keeping the same notation as for the 2D case for the coupling matrices  $M_1$  and  $M_2$ , the continuity of both the acoustic pressure and the component along the variable  $x$  of the displacement vector can be formulated in terms of the following system:

$$A + B = M_1 C \quad C = M_2 (A + B)$$

and

$$D_A A + D_B B = M_2 D_C C \quad D_C C = M_1 (D_A A + D_B B)$$

By defining  $R_1$  such that  $B=R_1 A$  and  $T_1$  such that  $C=T_1 A$ , similar calculations than in the 2D case give:  $R_1 = [I-D_B^{-1} M_2 D_C M_2]^{-1} [I-D_B^{-1} D_A] - I$  and  $T_1 = M_2 (I + R_1)$

In this way we can evaluate the reflected and transmitted acoustic field due to an incident plane wave (carried by one vertical mode) impinging a straight line bottom step with a grazing angle  $\theta_i$ . Two important remarks have now to be made:

1) The coefficients of the transmission and reflection matrices are depending on the grazing angle  $\theta_i$  and on the horizontal wave number  $\lambda_n$  associated with the vertical mode carrying the incident plane wave.

2) An horizontal incident plane wave (carried by only one vertical mode) always excites several different reflected and transmitted horizontal plane waves, each having their own propagation direction. Therefore, the treatment of even a simple configuration as one incident wave carried by  $n$  modes impinging one straight bottom step with a grazing angle  $\theta_i$  requires an important computing space and time because one have to add the contribution of  $n^2$  transmitted and reflected plane waves having their own propagation angle.

In order to reduce the complexity of this exponentially growing process, given that a large number of steps have to be considered in realistic situations, simplifying assumptions must be made. Analysing the structure of coupling matrices see ref [9], we can observe that an incident plane wave excites in transmission waves which may be classified into two parts: one associated with water to water and sediment to sediment transmission (ww-waves) and another one associated with water to sediment or sediment to water transmission (ws-waves). The "directions" of ww-waves may be interpreted as a spreading around the direction associated with the incident plane waves while the "directions" of ws-waves may be interpreted as a spreading around a direction which may be evaluated with the Snell law. For reflected waves, only a spreading around specular direction has to be considered. In MOCTESUMA 3D it is assumed that the direction associated with the transmitted field is the same than the one associated with the incident field and that in reflection, only the specular direction is considered. The advantage of this is the gain in CPU time (examples below). The main disadvantage of this method is that horizontal deviations due to bottom variations or sound speed variations are not taken into account.

In order to obtain more accurate results, we are currently testing a new version of the numerical code MOCTESUMA 3D. In this version, a new direction associated with the transmitted field is calculated at each encountered interface and for each incident plane wave. This direction is the one associated with the plane wave carried by the most excited mode in transmission. The advantage of this method lies in the fact that when the size of the steps used to describe the wave-guide tends to 0 it constitutes a good way to approximate the solution: one incident plane wave excites only one transmitted plane wave having its own propagating direction but, this approximation is valid only for small variations of the bathymetry and then, a large number of steps has to be used to correctly take into account variations of the bottom topography. In this case the CPU time needed may become prohibitive (see example below).

## V.2 Numerical results - Propagation over sinusoidal bottom with no horizontal deviation.

As a first example, we illustrate the possibilities of the two techniques described above in the case of transmission losses over a sinusoidal bottom. The bathymetry characteristics of the wave guide are the same as described in [11]. We consider a 25 Hz source at  $x=6$  km,  $z = 25$  m in a ocean the water depth of which is given by  $d = 50 (3 - \sin(0.002\pi x/6))$ . The water column and sea-bed are assumed to be homogeneous:  $c=1500$  m/s  $\rho=1$  in the water and  $c=1700$  m/s  $\rho=1.5g$  in the sediment.

In the paper published by Collins et al [11], comparisons between 3D and 2D parabolic equation (3DPE and 2DPE) at depth  $z=30$ m and for different azimuthal directions ( $\theta=40^\circ, 60^\circ, 80^\circ, 100^\circ, 120^\circ$  and  $140^\circ$ ) are presented. Due to horizontal coupling effects, most of the differences between 2DPE and 3DPE appear for  $\theta$  lying in interval  $[80^\circ, 100^\circ]$ .

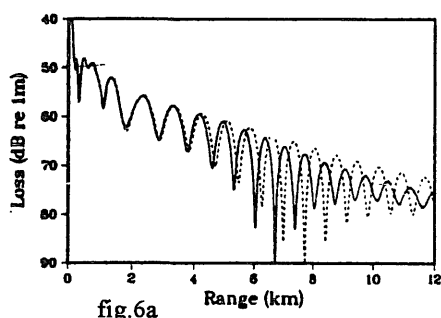


fig.6a

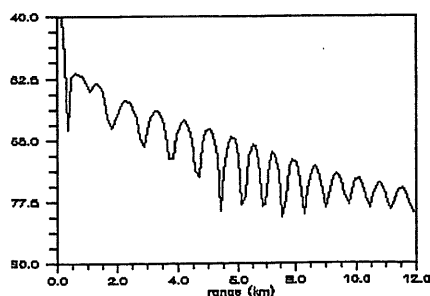


fig.6b

Figure 6 displays published results for  $\theta = 80^\circ$ : comparison between 3DPE (continuous curve) and 2DPE (dotted curve) while figure.6b displays results obtained with MOCTESUMA; calculating only the direct field and neglecting deviations in transmission. Here, the size of the steps used to describe bottom's variations is  $4m (\lambda/15)$ . The CPU time needed for running this version MOCTESUMA 3D in this configuration and using 40 modes amounts to 90 seconds for calculating modes families and coupling matrices on a SUN SPARK station 10. The mean time needed to calculate in each horizontal direction is 0.4 sec (depends on the number of encountered interfaces and in an area of  $24\text{km} \times 24\text{km}$  with 200 steps used to describe bottom's variations). Results concerning the total field (forward + backscattered-field) are not presented here because, in this configuration, the reflected field is negligible. In this case the CPU time needed for calculating the total field is approximatively 100 times the one needed for a calculation of the direct field in the complete area (when 200 steps are used to describe bottom's variations)

In this configuration, MOCTESUMA 3D gives results which converge to a solution between the two ones obtained with 2DPE and 3DPE. This result does not constitute a surprise because when the reflected field is negligible, the only differences between this version of MOCTESUMA 3D and 2D codes lies in the fact that the "amplitude" of the transmitted field evaluated with MOCTESUMA depends on the grazing angle of each incident wave impinging the bottom variations.

### V.3 Numerical results - Propagation over sinusoidal bottom with horizontal deviations.

In this section, the same wave guide as in the previous section (sinusoidal bottom) is considered; the numerical model used is an experimental one which introduces an horizontal deviation, at each isodepth encountered, by taking the direction of the most excited mode. Two points have to be underlined:

Assuming that a given source mainly excites  $N$  modes, CPU time needed for the calculation of the acoustic field is comparable to  $N$  times the one needed for calculating the acoustic field assuming that no significant deviations occur in transmission. In this case, in order to be sure that numerical results are convergent, the bottom topography has to be described with step functions small enough to remain in the framework of adiabatic approximation (on mode only excites one mode in transmission). As a consequence, the number of isodepth lines needed to describe the bottom topography might become such that the CPU time reaches unacceptable values. For example, calculation of the acoustic field over the sinusoidal bottom described above, in a square area ( $12\text{ km} \times 12\text{ km}$ ), with 200 steps to describe bottom variations (high of the steps  $2m = \lambda/30$ ), and using 30 modes need 30 h of CPU time on a SUN SPARK STATION 10.

Running this version of MOCTESUMA, we first have to notice that convergent results are difficult to obtain: horizontal coupling effects depend on the propagation direction of the incident wave. It is observed that convergent results relatively to the size of the steps used

to describe bottom's variation are more easy to obtain for azimuthal directions around  $\theta = 0^\circ$  than around  $\theta = 90^\circ$ . For example step size of 4m ( $\lambda/15$ ) is sufficient to obtain convergent results up to  $\theta = 30^\circ$  while up to  $\theta = 80^\circ$  step size of 2m ( $\lambda/30$ ) is necessary. Except for  $\theta = 80^\circ$  where small differences can be observed, this version of MOCTESUMA 3D gives results in good agreement with the ones published by Collins et al [11].

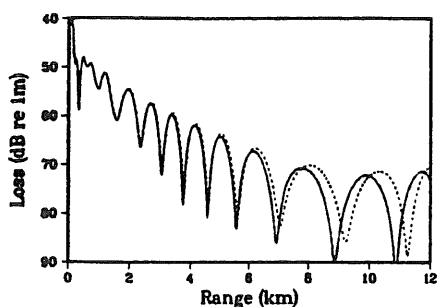


fig. 7a

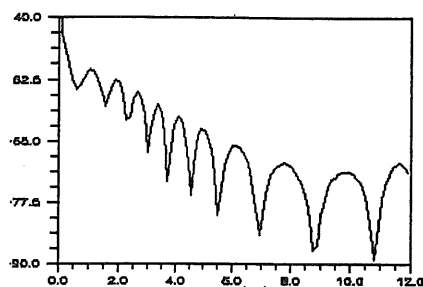


fig. 7b

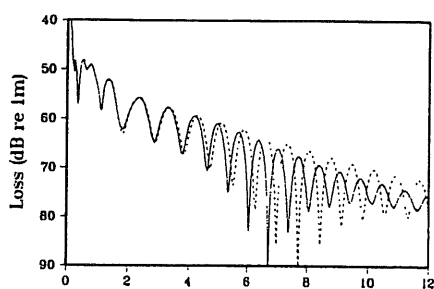


fig. 8a

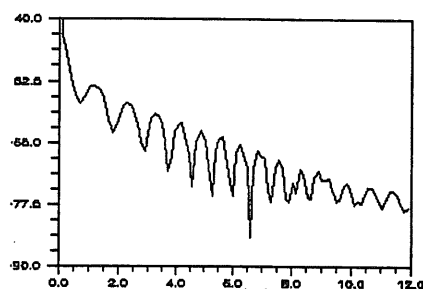


fig. 8b

Figures 7a and 8a display published results for  $\theta = 60^\circ$  and for  $\theta = 80^\circ$ : comparison between 3DPE (continuous curve) and 2DPE (dotted curve) while figure 7b and figure 8b display results obtained with MOCTESUMA. As it can be seen in figures 7a and 7b, differences between the two results are small. A possible way to explain these differences may be the following: for each mode and at each encountered interface, a new propagation direction is evaluated; due to the discretisation, once the direction of propagation is parallel to one of the isodepth lines used to describe the bottom's variations, no more deviation can numerically be obtained. This phenomenon is not realistic in cases of propagation over a continuous slope (see ref [13]). As an illustration of the horizontal deviations, figure 9 displays directions associated with the propagation of the second mode for two initial azimuthal angles.

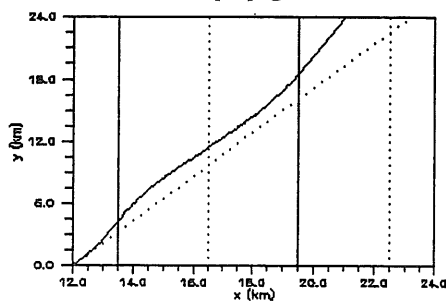
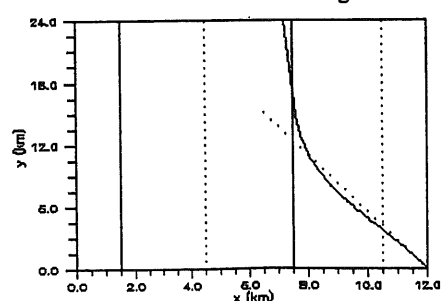
 $\theta = 65^\circ$ 

fig. 9

 $\theta = 110^\circ$

Figure 9: examples of horizontal deviations associated with the second mode.

In both cases, the source is located at  $x=12$  km and  $y=0$  km. Vertical lines display locations of maximum and minimum depths of the sinusoidal bottom (continuous curves are associated with 100 m depth and dashed curves with 200 m depth). The initial emission angle is displayed with a dashed curve.

## VI - CONCLUSION

This paper shows that it is possible to extend the Coupled Modes method to include the effect of shear in the sediment and to compute the backscattered field as well as the forward field including shear waves in range variable environment. Moreover the Galerkin method presented in this paper seems to be well adapted to take into account continuous variations with depth of compressional and shear velocities. In 2D cases, tests against other numerical codes indicate good behaviour of the TS.ASM Coupled Modes model called "MOCTESUMA". An important advantage of the Coupled Modes technique is found in the case of a moving source over a variable bottom; modal functions can be computed in advance for all possible water depths, and whatever the position of the source, the total field can be recovered very fast, without having to start again the whole computation, like with the Parabolic Equation technique.

In the 3D cases, results can be obtained with a reasonable CPU time provided assumptions are made on horizontal deviations. It is presently difficult to evaluate the validity of these assumptions since no reference result for low frequencies including forward and backward propagation effects is available yet. It is believed that the present scheme used to handle horizontal deviations is not well adapted to the case where the propagation direction is close to the bottom iso depth lines because once the modes direction is aligned with the bottom isodepth line, no more horizontal deviation can occur, which is of course not the case with a continuous bottom slope.

## REFERENCES

- (1) W.M. EWING, W. JARDETZKY and F. PRESS; *Elastic waves in layered media*. Mc Graw-Hill book company (1957).
- (2) L.M. BREKHOVSKIKH and Y. LYSANOV; *Fundamentals of ocean acoustics*. Springer-Verlag, Berlin (1982).
- (3) R.A. KOCH, C. PENLAND, P.J. VIDMAR, K.E. HAWKER; *On the calculation of normal group velocity and attenuation*. J. Acoust. Soc. Am. 73(3) 1983.
- (4) D.D. ELLIS and D.M.F. CHAPMAN; *A simple shallow water propagation model including shear wave effects*. J. Acoust. Soc. Am. 78(6) 1985.
- (5) B.A. AULD; *Acoustic waves and field in solids*. Wiley, New York, 1973; VOL II.
- (6) J. ARVELO and H. ÜBERALL; *A diabatic normal-mode theory of sound propagation including shear waves in a range-dependent ocean floor*. J. Acoust. Soc. Am. 88(5) 1990.
- (7) E. NOUTARY and X. CRISTOL; *A numerical coupled method for 3D acoustic propagation in oceans with immersion variations* in *European Conference on Underwater Acoustics*, ed. M. Weydert, Elsevier, 1992.
- (8) **MAST 2 - CT92 - 0019**; E.C project *PROMODE*, *oceanic acoustic propagation models*; First and Second year progress report.
- (9) **MAST - 0029 - CA**; *E.C project SNECOW*; Final technical report.
- (10) H. SCHMIDT, *SAFARI User's guide*, SACLANTCEN SR-113 (SACLANT Undersea Research Center, La Spezia, Italy, 1988).
- (11) M.D. COLLINS and S.A. CHIN-BING; *A three dimensional parabolic equation model that includes the effects of rough boundaries*. J. Acoust. Soc. Am. 78(6) 1985.
- (12) F.B. JENSEN and P. GERSTOFT "Benchmark solutions for backscattering in simple wave guide geometries" in *Proceeding of the second European Conference on Underwater Acoustics*, ed. L. BJORNO, ECSC-EC-EAEC, Brussels-Luxembourg 1994.
- (13) C.H. HARRISON; *Acoustic shadow zones in the horizontal plane*. J. Acoust. Soc. Am. 65(1) 1979.